Use of the advanced microwave sounding unit data to improve typhoon prediction

Guo Deng [a,*], Dalin Zhang [b], Tong Zhu [c], Angsheng Wang [d]

[a] National Meteorological Center, Beijing 100081, China
[b] Department of Atmospheric and Oceanic Science, University of Maryland, Maryland 20742, USA
[c] Cooperative Institute for Research in the Atmosphere, Colorado State University, Colorado 80523, USA
[d] Institute of Atmospheric Physics, Chinese Academy of Sciences, Beijing 100029, China

Abstract

The effects of incorporating the advanced microwave sounding unit (AMSU-A) data with a modified Zhu–Zhang–Weng vortex-bogussing algorithm on typhoon prediction are examined through the use of the PSU/NCAR Mesoscale Model version 5 (MM5). The AMSU-A data contain the vertical distribution of the retrieved temperature from satellite brightness temperature, with the geopotential height and wind fields derived through a series of statistical and diagnostic calculations. The advantages of the modified vortex-bogussing algorithm include the incorporation of realistic asymmetric typhoon structures, the balanced dynamics with the background field, the easiness to implement and the efficient computations. To test the efficiency of this vortex-bogussing algorithm, the Typhoon Dan event in 1999 is simulated by incorporating the derived AMSU-A fields into the initial conditions of the MM5 modeling system. Results show significant improvements in the track and intensity of the storm, as compared to the simulation without the AMSU-A data. Therefore, this modified vortex-bogussing algorithm can be easily implemented on any typhoon modeling system, which will improve the real-time forecast of tropical cyclones.
© 2008 National Natural Science Foundation of China and Chinese Academy of Sciences. Published by Elsevier Limited and Science in China Press. All rights reserved.

Keywords: AMSU; Satellite retrieval; Typhoon prediction

1. Introduction

Tropical cyclones (TCs) develop over the vast tropical oceans where few upper-air observations are available for numerical weather prediction (NWP). The lack of observations is one of the major limitations in determining the prediction of TCs. In most cases, operational analyses contain TC vortices that are either too weak or misplaced, or at too large scales. One has to ''bogus'' into the NWP model initial conditions of a TC vortex at the right location and with the right radius and realistic intensity in order to predict reasonably well its subsequent track and intensity.

Previous studies had shown that the proper incorporation of TC vortices into the model initial conditions could result in significant improvements in predicting their intensities and tracks, especially in the first 24 h. Some examples include the studies performed with the Geophysical Fluid Dynamics Laboratory hurricane model [1], the tropical cyclone-limited area prediction system (TC-LAPS) by the Australian Bureau of Meteorology Research Center [2], and with the model for typhoon track prediction (MTTP) at China's National Meteorological Center (NMC) [3]. However, most of the NWP models produce the TC vortices based on the experiential character of historical storms. Although these vortices exhibit some fundamental features of TCs, they do not contain realistic TC asymmetric structures. This is very important in TC simulations or forecasts

* Corresponding author. Tel.: +86 10 68400466; fax: +86 10 68407469.
  E-mail address: deng719@cma.gov.cn (G. Deng).

because the dynamical and thermodynamic asymmetric structures could affect the movement and intensity of TCs [4]. In fact, we have not yet observed two TCs that share the same track and the same radar reflectivity structures. Besides the synthetic TC structures, the other shortcomings in the traditional bogussing methods may include the limited observational data used and the initialization problem associated with inserting bogussed TCs. Therefore, it is desirable to provide more realistic representations of TC vortices for NWP models, which include observation data as many as possible.

In this regard, Zhu et al. [5] developed an effective algorithm to retrieve hurricane vortices hereafter referred to as the Zhu–Zhang–Weng (ZZW) algorithm based on the statistical relationship between the advanced microwave sounding unit (AMSU-A) data and the vertical distribution of temperature. The ZZW algorithm was successfully tested with a single TC, i.e., Hurricane Bonnie (1998) at its early stage, over the Atlantic Ocean. Because of the successful simulation, the model data were later analyzed to gain insight into various physical processes leading to different aspects of the storm, such as the partial eyewall, the eyewall replacements and the effects of sea-level temperature [5–7].

Although their results are encouraging, it is unclear to what extent the same algorithm could be applied to other TCs, especially those occurring over the West Pacific where even fewer real-time observations are available. Furthermore, it would be even a more severe test of the algorithm in spinning up the right storm intensity when it is applied to the mature stage of a hurricane/typhoon. Still further, we wish to simplify the ZZW algorithm and make it computationally more efficient by excluding the divergent wind component, because it is small compared to the balance flow and because it may propagate away quickly in the form of inertial gravity waves once the model integration begins. Thus, the purpose of this study is to apply this modified ZZW algorithm to a mature typhoon that occurred over the West Pacific Ocean, and to test it through a pair of numerical model simulations, in which the modified ZZW algorithm is turned on and off to see its effectiveness and efficiency in predicting the storm.

2. Methodology

The AMSU instrument on the NOAA-15 satellite contains two modules: A and B. The A module (AMSU-A) has 15 channels and is mainly designed to provide information on atmospheric brightness temperature profiles, and the B module (AMSU-B) allows for the profiling of the moisture field. The ZZW algorithm contains a detailed description of the AMSU-A data. Briefly, the AMSU-A measures the thermal radiation at microwave frequencies ranging from 23.8 to 89.0 GHz. In particular, the AMSU-A sounding channels (3–14) respond to the thermal radiation at various altitudes because of their weighting

function distributions (see Fig. 1). Because microwave radiance responds linearly to temperature and the weighting functions at various AMSU sounding channels are relatively stable, the temperature at any pressure level can be expressed as a linear combination of brightness temperatures measured at various sounding channels (see Ref. [8]), i.e.,

$$T(p) = C_0(p, \theta_s) + \sum_{i=1}^{n} C_i(p, \theta_s) T_b(v_i, \theta_s) \qquad (1)$$

where p is the pressure; θ_s is the scanning angle; v_i is the frequency at channel i; and T_b is the AMSU brightness temperature. The coefficients C_0 and C_i are determined by a regression equation, in the same form as Eq. (1), which matches the rawinsonde temperature soundings with the AMSU-A brightness temperatures at the co-located tropical islands (see ZZW for more details).

Now, let us examine how well this algorithm performs in retrieving the 3D temperature structures at the mature stage of Typhoon Dan which occurred at 0000 UTC 6 October 1999, which is also the time used to initialize the simulations of the storm. Fig. 2(a) shows a vertical cross section of the temperature anomaly at the mature stage (in σ-coordinates, the temperature anomaly is defined herein as a deviation from the unperturbed environmental temperature) during which the storm's track begins to turn from westward to northward (see Fig. 3). Apparently, a warm core can be identified throughout the troposphere with a maximum value of over 8 °C at the upper level. In contrast, the maximum anomaly from the European medium-range weather forecast (ECMWF) analysis is only slightly larger than 4 °C (Fig. 2(b)). This anomalous structure is much weaker than that typically observed in
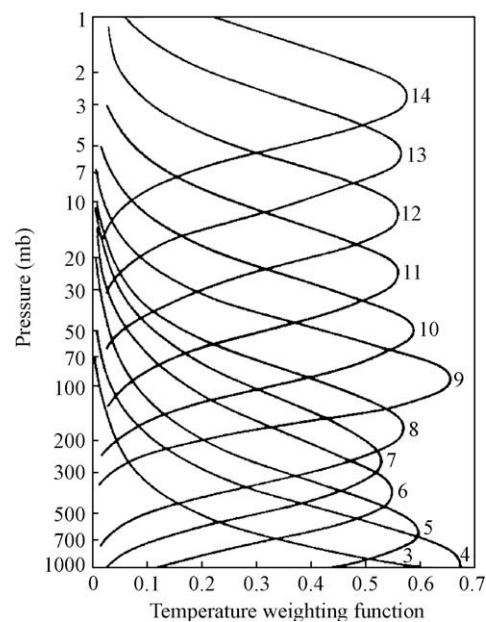
Fig. 1. Vertical distribution of the AMSU-A channels 3–14 weighting function at nadir over land (adapted from Janssen [8]).
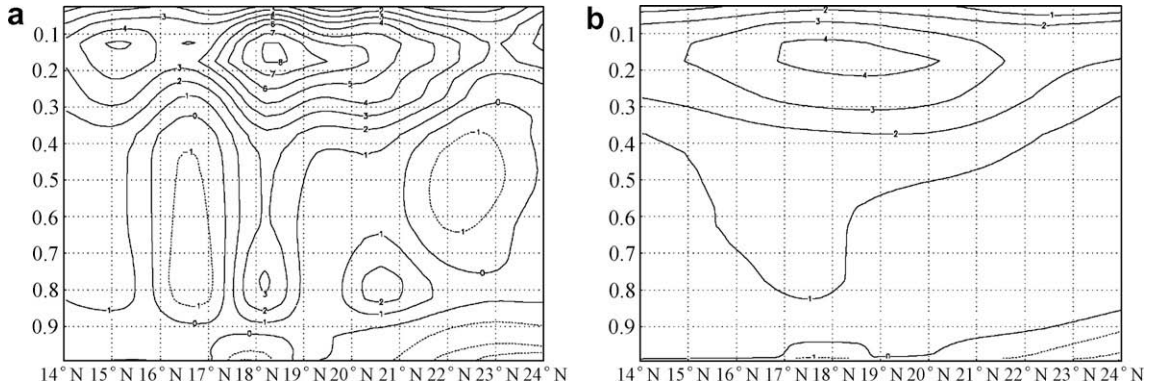
Fig. 2. South–north vertical cross sections of temperature anomalies (every 1 °C) associated with Typhoon Dan at 0000 UTC 6 October 1999 along the longitude of 118°E. (a) From the bogussed AMSU-A data and (b) from the ECMWF analysis.
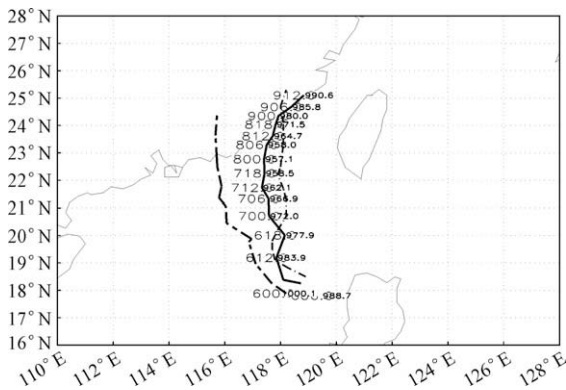
Fig. 3. A comparison of the tracks of Typhoon Dan (1999) from the AMSU (dot dashed) and sensitivity (long dashed) simulations to the best track analysis (solid). The positions of the storm centers are given every 6 h.

TC warm-core structures [9]. To avoid possible cold anomalies associated with contamination by the thermal emission of large cloud droplets, only the cleaner AMSU-A channels (i.e., 6–11) were used to retrieve the temperatures in the regions of heavy precipitation, e.g., in the eye-wall. Otherwise, if we used channels 3–11, the warm-core magnitude could reach 9–10 °C, but with a cold anomaly of 4 °C at the lower level of the retrieved atmosphere as a result of the heavy rainfall contamination below 700 hPa.

It is evident that the retrieval method presented above could be used to obtain the temperature profile, especially in the eye region of typhoons. However, when the retrieved temperature field is compared to the large-scale ECMWF analysis, there will be some obvious differences between the two data, both at the typhoon core and at the lower levels (i.e., below 700 hPa), as mentioned above. So, care needs to be taken in using the retrieved low-level temperature field. In this study, we combined the background fields with the temperature anomalies obtained from the above retrieval method through the following two steps: (i) the detection and extraction of a TC from the first-guess fields and (ii) the blending of the AMSU-retrieved temperature field with the modified background field.

There are several approaches that we could take to obtain the background fields. In the present study, we adopted the method developed by Davis and Low-Nam, the NCAR-AFWA tropical cyclone Bogussing scheme, a report prepared for the Air Force Weather Agency (AFWA), 2001. Unlike the usual filtering methods, Davis and Low-Nam's method can help minimize some adverse effects on the far field in separating a TC vortex from the background fields. Specifically, after identifying the vortex associated with the storm of interest by searching for the maximum relative vorticity at the pressure level next to the surface in the analysis field (e.g., either 1013 or 1000 hPa), we can remove the temperature anomalies from the first-guess fields using the hydrostatic relationship as follows:

$$\frac{\partial \phi'}{\partial \ln(p)} = -RT' \qquad (2)$$

where R is the gas constant and p is the pressure, while ϕ' and T' indicate temperature anomaly and geopotential height anomaly, respectively. The next step is to add the AMSU-retrieved temperature anomaly into the first-guess fields, which will be referred to as the bogussed AMSU temperatures. In this way, we are able to obtain the "bogussed" 3D temperature field that contains information from both the background and the AMSU-A data.

With the bogussed temperature, the hydrostatic equation can be integrated from either the bottom upward or the top downward to obtain the geopotential height field. Herein, we use the bottom upward approach as was done by ZZW. To reasonably prescribe the bottom boundary conditions, we adopt the scheme of Holland [10] that requires knowledge of the surface maximum wind (V_{MAX}), RMW (R_{MAX}) and the minimum central pressure (P_{CEN}) from routine observations. In this study, we took $P_{CEN} = 970$ hPa, $R_{MAX} = 90$ km and $V_{MAX} = 35$ m s^{-1} based on the best track analysis. With the specified sea-level pressure (SLP) field, the geopotential field at all pressure levels could be computed using the AMSU bogus temperatures. A comparison of the geopotential height field so obtained to that from the ECMWF analysis is given in

Fig. 4, which shows a deep vortex and a relatively shallow system at the center. Clearly, the deep vortex structures represent more realistically the storm of interest.

After obtaining the temperature and geopotential height fields, one can obtain the pertinent 3D rotational winds using the (gradient) balance equation [11] in terms of geopotential height (φ) and stream function (ψ):

$$f\nabla^2\psi + 2\left(\psi_{xx}\psi_{yy} - \psi_{xy}^2\right) + \psi_x f_x + \psi_y f_y = \nabla^2\phi \qquad (3)$$

where f is the Coriolis parameter, and ∇ is the two-dimensional gradient operator. Solving the stream function ψ from the given geopotential ϕ using the successive over-relaxation (SOR) method is a Monge-Ampere type of problem, as long as an ellipticity condition is satisfied. ZZW showed that the ellipticity condition could be easily satisfied in hurricanes/typhoons. In this study, the lateral boundary conditions for ψ were specified from the ECMWF's global $2.5° \times 2.5°$ analysis, assuming that the domain-averaged divergence vanishes. The successive over-relaxation method was then adopted to solve Eq. (3) for ψ. The first guess for ψ was assumed to be zero everywhere in the domain except at the lateral boundaries.

After obtaining the stream function over the computational domain, the 2D horizontal wind vector field can be calculated easily from

$$\mathbf{V} = \mathbf{k}X\nabla\psi \qquad (4)$$

where $\mathbf{k}$ is the vertical unit vector. As compared to the ZZW algorithm, the divergent wind component is not included, as mentioned before. To see the effectiveness of the retrieved flow fields from the AMSU-A data, Fig. 5 compares the 500 hPa horizontal winds between the ECMWF analysis and the bogussed AMSU field at 0000 UTC 6 October 1999. One can see that the wind structures from the two datasets are very similar in general, i.e., the maximum wind speed is located in the northern part of the typhoon, and the wind speed is small at the center. But one can also see that the retrieved wind speed is much stronger than that of the large-scale analysis, and is very close to the observed wind speed.

3. Numerical simulations

3.1. Model description and initial conditions

To test the effects of incorporating the AMSU data on the simulation of TCs, a double nested, two-way interactive version of the PSU/NCAR MM5 (v3.5) was used [12,13]. The two domains had the (x, y) dimensions of 140×130 and 169×163 grid points, with the grid sizes of 36 and 12 km, respectively. There were 26 σ-levels in the vertical, which were placed at 1.0, 0.995, 0.985, 0.975, 0.965, 0.945, 0.930, 0.905, 0.87, 0.825, 0.775, 0.675, 0.625, 0.575, 0.525, 0.475, 0.425, 0.375, 0.325, 0.275, 0.225, 0.175, 0.125, 0.075, 0.025, and 0. Considering the use of different horizontal resolutions in the two domains, different physics parameterization schemes were used. Namely, in the coarse-mesh domain, a simple ice-microphysics scheme was used together with the Grell [14] cumulus parameterization scheme, while in the fine-mesh domain the Reisner et al. [15] cloud microphysics scheme with the mixing ratio of graupel included and the Betts–Miller [16] cumulus scheme were simultaneously used. The two domains use the same schemes for all the other physical processes, e.g., the Burk–Thompson [17] planetary boundary layer scheme, a cloud-radiation interaction scheme and a shallow convective scheme [14].

The initial conditions at 0000 UTC 6 October 1999 were obtained from the ECMWF's $2.5° \times 2.5°$ global analysis data, and then integrated for 72 h, validated at 0000 UTC 9 October 1999. To see the effects of bogussing a typhoon vortex into the model initial conditions, two different numerical simulations of Typhoon Dan (1999) were performed with the MM5 model (referred to as the AMSU) and sensitivity runs, respectively. In the AMSU run, the initial typhoon vortex was obtained using the procedures described in Section 2 and placed at the central portion of the coarse-mesh domain (about 1400 km $\times$ 1400 km); the fine-mesh domain data were interpolated from its mother domain. Note that the vortex-bogussing was performed in the coarse-mesh domain because the resolution
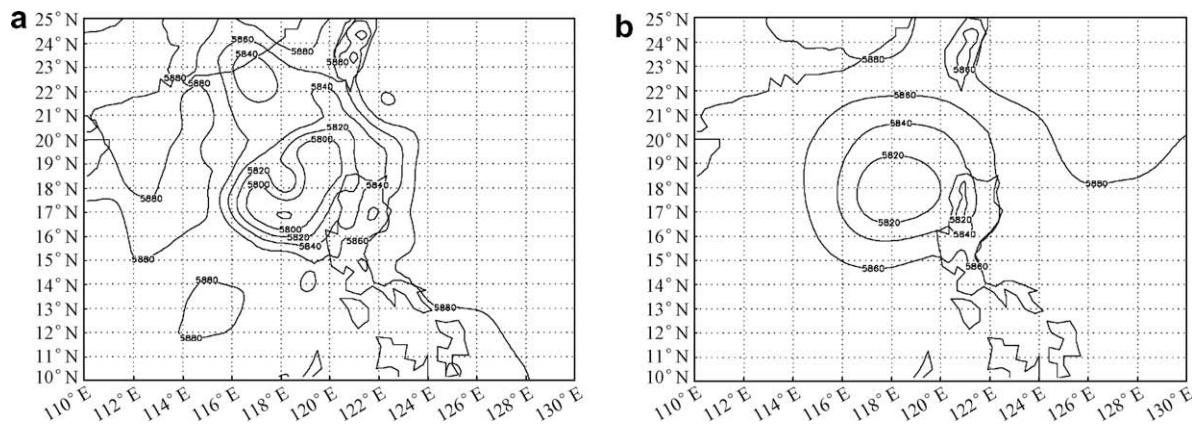
Fig. 4. The 500 hPa geopotential height at 0000 UTC 6 October 1999. (a) From the bogussed AMSU-A data and (b) from the ECMWF analysis.
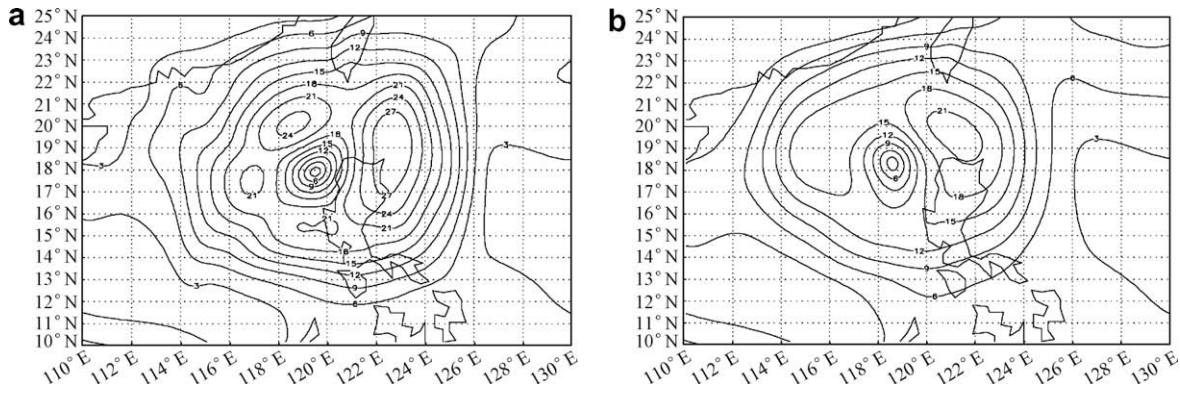
Fig. 5. The 500 hPa horizontal wind speeds at 0000 UTC 6 October 1999. (a) From the bogussed AMSU-A data and (b) from the ECMWF analysis.

of the AMSU-A data was about 48 km which is even greater than the 36 km coarse-mesh resolution. In the sensitivity run, the ECMWF analysis was used as the initial conditions for the two domains. Different results of the storms obtained from the two simulations could reveal the effects of incorporating the AMSU-A data in TC prediction.

3.2. Numerical simulations

Fig. 3 compares the tracks of Typhoon Dan from the two 72 h simulations to the best track analysis (i.e., the observations). By incorporating the AMSU data, the storm could be placed at the right location to begin with. It is obvious that the track of the AMSU run is much closer to the observed than the sensitivity test. The difference in track between the sensitivity run and the best track becomes larger with time, and it exceeds 3° (i.e., 300 km) to the west of that observed at 60 h into the integration. In contrast, the track of the AMSU run keeps close to that observed during the 72 h simulation, and the largest departure is no more than 1°.

The simulated minimum central pressures are compared to the best track analysis in Fig. 6, which shows that the AMSU run is better than the sensitivity run at most time.
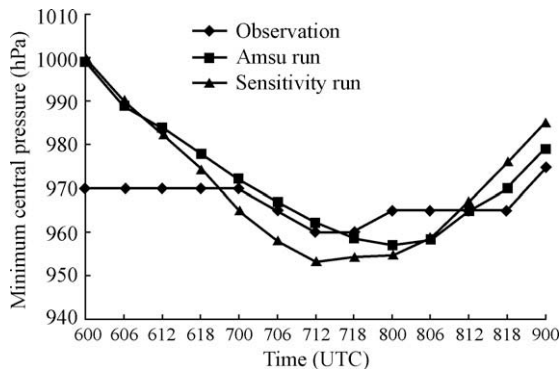
Fig. 6. Time series of the minimum central pressure (in hPa) from the observed (diamond), the AMSU (rectangle) and sensitivity (triangle) simulations between 0000 UTC 6 and 0000 UTC 9 October 1999.

The minimum sea-level pressure at the 36 h integration of the sensitivity run is 7–8 hPa which is lower than that at both the AMSU run and the observation, even it starts from a smoother analysis field. Similarly, the maximum surface wind from the bogussed AMSU run is closer to that observed at the initial time, because of the incorporated AMSU data. As the time passes by, the bogussed AMSU run keeps well with the observed maximum surface winds. By comparison, the sensitivity run is much weaker than that observed to begin with, but its subsequent spin-up accelerates and the simulated storm becomes much stronger than that observed at the later times. Of interest is that after 1200 UTC 8 October, the maximum wind speed weakens at a rate faster than that observed. This more rapid weakening appears to be attributable to the relatively drier larger-scale environment to the west in which the storm moves.

Since Reisner's cloud microphysics scheme could output the mixing ratios of rain water, cloud ice crystal, snow, and graupel, the simulated cloud images between the AMSU run and the observed infrared images were also compared. We found quite good agreements between the AMSU run and the observations in terms of the general cloud distribution in the eyewall and spiral rainbands.

In summary, the simulation with the bogussed typhoon vortex exhibits a considerable skill in reproducing the observed track, intensity and inner-core structures of the storm. In particular, the simulated asymmetry in the precipitation structure has important applications with respect to the improvement of quantitative precipitation forecasts and severe wind warnings for landfalling typhoons. Without the AMSU data incorporated (i.e., in the sensitivity run), the simulated intensity and cloud structures differ markedly from the observed.

4. Discussion

In this section, we will attempt to provide an understanding of why incorporating the AMSU-A data using the modified ZZW vortex-bogussing algorithm could help improve the simulation of Typhoon Dan (1999) or gener-

ally TC forecasts even in an operational setting. Previous studies had shown that the horizontal cloud and flow structures of TCs could have significant effects on their tracks and precipitation distribution [18]. However, most of the traditional vortex-bogussing schemes produce TC vortices either empirically or based on the previous TC observations, or simply by modifying the large-scale first-guess fields. Thus, with these methods NWP models would often fail to represent realistically TC vortex structures, accounting partly for the predicted errors in track and intensity of TCs. Of course, larger-scale flows also play important roles in determining the track and intensity of TCs.

As shown above, the modified ZZW vortex-bogussing algorithm could reproduce the 3D fields of temperature, horizontal winds, and geopotential heights reasonably well for initializing NWP models; and it is mainly limited by the resolution of the AMSU-A data as well as the heavy rainfall contaminations. We can see from Fig. 2 that the retrieved AMSU-A data exhibit a typical warm-core structure at the typhoon central region at the initial time, which is much stronger than that of the ECMWF analysis. As a result, the perturbation geopotential height field is deeper than that in the ECMWF analysis (Fig. 4), with the tangential winds closer to that observed (Fig. 7). This indicates that accurate representation of this thermal structure in the eye regions of TCs is critical to the realistic generation of the minimum sea-level pressure and the low-level cyclonic rotational winds through the thermal wind relation. In this regard, Davidson and Puri [19] used the satellite-derived latent heat release in the eyewall to help spin up a hurricane vortex, and showed a positive impact on hurricane forecasts for up to 48 h. In addition, use of the AMSU-A data will help correct any errors in the initial positions of TCs, as shown in Fig. 3, which would assist in the prediction of their subsequent movements.

Unlike the other vortex-bogussing algorithms, the modified ZZW algorithm could retrieve detailed information at the resolution of the AMSU-A observations though currently at 48 km. This is higher than the resolution of the existing large-scale analyses of more than 100 km, and can provide some useful information to spin up mesoscale
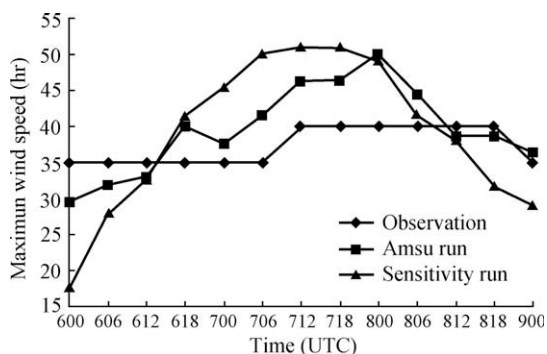
flow features in NWP models. These mesoscale flow features could interact with some microphysical processes to influence the development of cloud convection and precipitation in TCs as well as the storm intensity. Similarly, they may also interact with the larger-scale flows to affect the track and intensity of the storms. All the above features help explain why the bogussed AMSU run performs better than the sensitivity run, as shown in Figs. 3, 6 and 7.

The spin-up concept is another important issue of TC forecasts with NWP models in general. In the sensitivity run, which utilizes the large-scale ECMWF analysis as the initial conditions, the model spin-up typically requires a long-time period to attain the observed intense tangential winds that are in balance with the mass field. This could only be achieved by reproducing reasonably clouds and precipitation in order to catch up with the storm intensity through the nonlinear interaction with the larger-scale flows and latent heat release. In contrast, in the bogussed AMSU run, the retrieved fields of temperature, geopotential height and wind, are dynamically consistent and close to that observed, and they have already contained some important mesoscale features to begin with. Thus, the model spin-up time of the bogussed AMSU run would be much shorter than that of the sensitivity run, for the same given moisture field. These features can also be seen from Figs. 3, 6 and 7.

Finally, we like to mention that remote-sensing data from satellite observations will play an increasing role in NWP for many years to come, particularly for TCs developing in the vast tropical oceans where little upper-air observations are available. Data retrieval and (3D and 4D) data assimilation of satellite radiance are the two typical approaches for incorporating the satellite data into NWP models. Although data assimilation has been more widely used than data retrieval in many operational NWP centers, there are still some advantages with the use of the data retrieval approach, particularly as applied to the AMSU data. First, the correlation between the AMSU-A brightness temperature and the atmospheric temperature is well behaved, even in the presence of (non-precipitation) clouds. In the data retrieval approach, the linear correlation coefficients that we use to retrieve temperature are obtained by matching the AMSU-A brightness temperatures with many co-located rawinsonde temperature soundings over tropical islands. The data retrieval procedures are straightforward and easy to implement, and the retrieval accuracy is comparable to that of rawinsonde observations in the upper troposphere (see ZZW).

By comparison, it is necessary to specify both the background error covariance and the observation error covariance in order to obtain more realistic initial conditions through the data assimilation. Because these error covariances need to be attained over the entire model domains rather than simply the TC area of interest, it is difficult to obtain accurately the 3D flow structures of the TC, besides the difficulties that arise in defining the error covar-

Fig. 7. Time series of the maximum wind speed from the observed (diamond), the bogussed AMSU (rectangle) and sensitivity (triangle) simulations between 0000 UTC 6 and 0000 UTC 9 October 1999.

iances. Second, retrieving the temperature and the wind fields from the satellite radiance is more efficient than the 4D data assimilation that requires many back and forth iterations using NWP models. Assimilating all possible remote-sensing data and other non-conventional observations with the existing NWP models are indeed computationally expensive with today's computer power, or even when considering the continued growth of computing power for the next few years. Thus, the data retrieval approach to process the AMSU-A data still appears to be a good option for some researchers and operational forecast centers.

5. Summary and conclusions

In this study, the modified ZZW vortex-bogussing algorithm for incorporating the AMSU-A data into the model initial conditions was presented and then tested with the numerical simulations of Typhoon Dan using the PSU/NCAR mesoscale model. In this algorithm, the atmospheric temperature profile was first retrieved statistically from the AMSU-A sounding channels of brightness temperature, based on the co-located upper-air observations over tropical islands. Then, the geopotential heights were obtained by integrating the hydrostatic equation from the bottom upward with the retrieved temperatures. The associated horizontal wind field was derived from the nonlinear balance equation using the ECMWF analysis as the lateral boundary conditions.

It was found that the retrieved temperature, geopotential height and wind fields exhibited the same background as the ECMWF analysis, but contained some useful mesoscale structures, including some flow asymmetries, associated with Typhoon Dan. Because of the use of the background flow as the lateral boundary conditions, the retrieved mass and wind fields could be incorporated into the model initial conditions with little "discontinuity". In addition, because the AMSU-derived mass and wind fields are dynamically consistent, this modified ZZW algorithm provides an objective, observation-based way to incorporate a typhoon vortex with reasonable asymmetries into the initial conditions of TC models.

Two 72 h simulations of Typhoon Dan were performed with the MM5 model to examine the effectiveness of using this vortex-bogussing algorithm in reproducing the observed track, intensity and structures. Results showed that with the incorporation of the AMSU data, the simulated intensity and cloud structures of Typhoon Dan were very close to the observations, whereas without the AMSU data these zero-order variables differed markedly from that observed. In addition, the model produced a track error of more than 300 km at the end of the 72 h simulation in the absence of the AMSU data.

Finally, it should be mentioned that the modified ZZW algorithm appears to have retrieved a warm-core TC vortex that is more intense than that in the large-scale analysis. Some rotational structures also appear to differ from those

typical hurricanes. These differences may be attributed to the different environment in which Typhoon Dan developed, as compared to Hurricane Bonnie (1998) that occurred over the Atlantic Ocean. To resolve this issue, it is necessary to obtain a different set of the correlation coefficients as required by the regression equation (1), following Zhu et al. [5], by matching the AMSU-A sounding data with more upper-air rawinsonde observations over the West Pacific Ocean. This will remain part of our future research to improve the representation of typhoon vortices taking place over the region.

References

[1] Kurihara Y, Bender MA, Tuleya RE, et al. Improvements in the GFDL hurricane prediction system. Mon Wea Rev 1995;123(9):2791–801.

[2] Davidson NE, Weber H. The BMRC high-resolution tropical cyclone prediction system: TC-LAPS. Mon Wea Rev 2000;128(5):1245–65.

[3] Qu A, Ma S. The design of asymmetric bogus vortex scheme and preliminary experiment. J Appl Meteo Sci 2007;18(3):380–7 (in Chinese).

[4] Chen L, Xu X, Luo Z, et al. Introduction to tropical cyclone dynamics. Beijing: China Meteorological Press; 2003, p. 92–146 (in Chinese).

[5] Zhu T, Zhang D, Weng F. Impact of the advanced microwave sounding unit measurements on hurricane prediction. Mon Wea Rev 2002;130(10):2416–32.

[6] Zhu T, Zhang D, Weng F. Numerical simulation of Hurricane Bonnie (1998). Part I: eyewall evolution and intensity changes. Mon Wea Rev 2004;132(1):225–41.

[7] Zhu T, Zhang D. Numerical simulation of Hurricane Bonnie (1998). Part II: sensitivity to varying cloud microphysical processes. J Atmos Sci 2006;63(1):109–26.

[8] Janssen MA. Atmospheric remote sensing by microwave radiometry (Wiley series in remote sensing). New York: Wiley; 1993, p. 572.

[9] Hawkins HF, Rubsam DT. Hurricane Hilda, 1964. Mon Wea Rev 1968;96(9):617–36.

[10] Holland GJ. An analytic model of wind and pressure profiles in hurricanes. Mon Wea Rev 1980;108(8):1212–8.

[11] Shapiro LJ, Willoughby HE. The response of balance hurricanes to local sources of heat and momentum. J Atmos Sci 1982;39(2):378–94.

[12] Grell G, Dudhia J, Stauffer D. A description of the fifth-generation Penn State/NCAR Mesoscale Model; NCAR/TN-398+STR; 1995.

[13] Zhang D, Chang H, Seaman NL, et al. A two-way interactive nesting procedure with variable terrain resolution. Mon Wea Rev 1986;114:1330–9.

[14] Grell G. Prognostic evaluation of assumptions used by cumulus parameterizations. Mon Wea Rev 1993;121:764–87.

[15] Reisner J, Rasmussen RM, Bruintjes RT. Explicit forecasting of supercooled liquid water in winter storms using the MM5 mesoscale model. Quart J Roy Metero Soc 1998;124B:1071–107.

[16] Betts AK, Miller MJ. The Betts–Miller scheme: the representation of cumulus convection in numerical models. Am Meteor Soc 1993: 246.

[17] Burk SD, Thompson WT. A vertically nested regional numerical prediction model with second-order closure physics. Mon Wea Rev 1989;117:2305–24.

[18] Gao S, Ping F, Li X. Cloud microphysical processes associated with the diurnal variations of tropical convection: a 2D cloud resolving modeling study. Meteor Atmos Phys 2006;91(1):9–16.

[19] Davidson NE, Puri K. Tropical prediction using dynamical nudging, satellite-defined convective heat sources, and a cyclone bogus. Mon Wea Rev 1992;120(11):2501–22.